Synthesis of Cr and Al Substituted Calcium Nano Hexaferrites by sol – gel Auto-combustion Method.

B. S. Satone[1], K. G. Rewatkar[2], A.S.Kakde[2], P. S. Sawadh[3], M.S. Choukuse[4].

[1] Department of Physics, S.H.J.C., Nagpur.
[2] Department of Physics, Dr. Ambedkar college, Nagpur.
[3] Department of Applied Physics, Baburao College of Engineering, Sewagram, Wardha.
[4]Department of science and Humanities, Govt. Engineering College, Ponda, Goa.

Abstract

In the present research module the samples with chemical composition $CaMeFe_{11}O_{19}$ (where Me = Al and Cr) were successfully synthesized using perfect stoichiometeric proportions of reacting oxides by sol gel auto-combustion method. X - ray diffraction analysis of sample showed that both the compounds are in single, hexagonal M - type phase with unit cell dimensions 'a' and 'c' varies between 5 to 6 Å and 21 to 23 Å respectively with space group SG:$P6_3/mmc$ (No. 194). Scanning Electron Microscopy (SEM) analysis showed a good crystallization, smooth surface without any cracks. The Transmission Electron Microscopy (TEM) analysis proved that the compounds belong to nanoparticle range. The magnetic properties measured using vibrating sample magnetometer (VSM), optimized saturation magnetization (Ms) of the compound reached 67.9emu/g and 14.8emu/g for Al and Cr substituted compound respectively, while coercive force (Mr) ranges between 3386.1 Oe for Al and 1046.0 Oe for Cr. These values are close to that of its counterpart CaM.

Keywords: Nanoferrite, Saturation magnetization, Coercivity, Sol gel auto combustion, X – ray diffraction, etc.

1. Introduction

Ferrites continued to attract attention of researchers over the years due to their broad category of applications over wide frequency range, low cost and high performance. They are found suitable in microwave devices, memory core, perpendicular magnetic recording and permanent magnets. These applications need significant magnetic and electrical specifications and in this view, several attempts have been made to modify the properties of hexagonal ferrites using different processing route including external doping [1- 4]. Recently the research on ferrite have been shifted towards developing ferrites at nanometric scale due to its unique mechanical, electrical, optical and magnetic properties. The unique property of nanostructure materials are due to changed electronic structure closed to that of isolated atom or molecule [5].

The magnetic properties of hexagonal ferrites depend on the intrinsic magnetic properties of the naturally occurring magnetoplumbite (M-type) crystal ferrite phase. The structure of M-type ferrite phase is hexagonal in nature having 64 ions per unit cell on 11 different symmetry sites. The 24 Fe^{+3} atoms are distributed over five distinct sites: three octahedral sites (12k, 2a and $4f_2$), one tetrahedral site ($4f_1$) and one bipyramidal site (2b). The magnetic structure given by the Gorter coollinear spin model [6] in the ferrimagnetic with five different sub-lattices, three parallel (12k, 2a and 2b) and two anti-parallel ($4f_1$ and $4f_2$) which are coupled by super-exchange interactions through the O^{-2} ions [7-9]. The intrinsic magnetic properties of M-type ferrites can be improved by partial

substitution of Co, Cr , Al ,Fe or all [10], meanwhile our work [11] has shown that Co and Zr additives to CaM produce significant improvement in magnetic parameters viz. coercivity, saturation magnetization, and magnetic remenance. In order to extend this investigations in this research module sol gel auto combustion is used, as this route provides a good control over the particle size, assures higher homogeneity of particles, more sustained electric and magnetic properties and produce samples in relatively short time.

In this paper, $CaMeFe_{11}O_{19}$ (where,Me =Al & Cr) nanoparticle samples were reported with structural, morphological and magnetic behaviour of these materials compared with those of CoZr, SnZr substituted samples reported earlier [12].

2. Experimental details

The nanoparticles of $CaMeFe_{11}O_{19}$ (where Me = Al and Cr) have been synthesized by sol gel auto-combustion method. The stoichiometeric proportions of AR grade compounds of calcium nitrate $[Ca(NO_3)_24H_2O]$, iron nitrite $[Fe(NO_3)_39H_2O]$, chromium nitrite $[Cr(NO_3)_39H_2O]$ and aluminium nitrite $[Al(NO_3)_39H_2O]$ were taken for preparation of samples, while the urea $[Co(NH_2)_2]$ was used as the fuel. The mixture of precursor were dissolved in deionized triple filtered water. The solution was then allowed for gel formation by slow drying process, which was converted in to dense ceramic material under calcination of 60 – 70 ^{0}C.

The gel formed was fired in specially designed microwave, yielding powder ash, which was followed by grinding for about 5 hours so that fine powder of nanosized particles was prepared. The resulting powder were heated in electric furnace up to 800 ^{0}C for about 8 hours by increasing temperature slowly to remove any residual organic impurity present in the sample and then cooled at the same rate. The powder samples of all the specimens were then subjected to the characterization.

3. Result and Discussion:

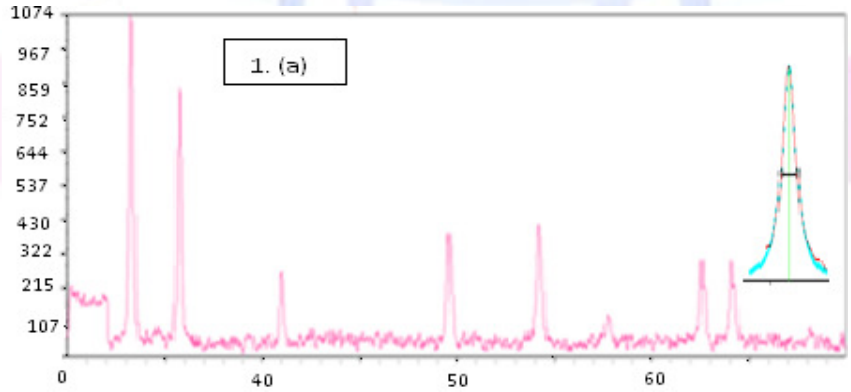

Fig:1a shows XRD pattern and Broadening of respective high intensity peak for $CaAl_1Fe_{11}O_{19}$

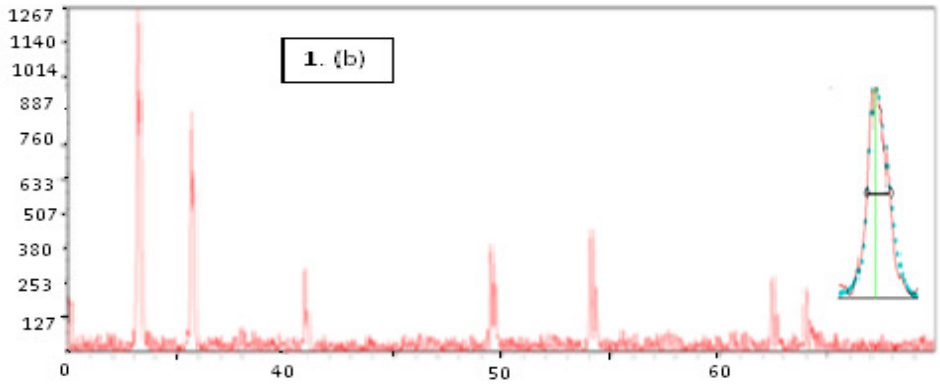

Fig:1b shows XRD pattern and Broadening of respective high intensity peak for $CaCr_1Fe_{11}O_{19}$

Table No. 1: Structural data

Name of sample	a (Å)	c (Å)	a/c	ρ_X Kg/m^3	ρ_M Kg/m^3	Porasity	Partical size D nm
$CaAl_1Fe_1O_{19}$	5.811	22.0350	0.2631	$5.0642x10^3$	$2.2038x10^3$	0.6957	43 nm
$CaCr_1Fe_{11}O_{19}$	5.811	22.0412	0.2637	$5.2020x10^3$	$3.3529x10^3$	0.3554	52 nm

Table No. 2: Comparative 'd' values of the samples

h k l	d - values in Å of the samples	
	$CaAl_1Fe_{11}O_{19}$	$CaCr_1Fe_{11}O_{19}$
1 1 3	2.7044	2.7015
1 0 7	2.6696	2.6670
2 0 0	2.5190	2.5163
2 0 1	2.5027	2.5000
0 0 12	1.8363	1.8345
3 0 4	1.6064	1.6047
2 2 0	1.4544	1.4528

Figure 1 (a) and (b) shows X-ray diffraction for Ca – Hexaferrites samples synthesized by sol gel auto combustion technique as described earlier [2, 10]. The diffraction peaks indicated in the figure corresponds to pure calcium hexaferrites. The table no. 1 summarizes various parameters concerned with structural data and table no. 2 depicted comparative'd' values of the samples. All the reflections can be indexed applying hexagonal crystal system and space group SG: $P6_3/mmc$ (NO. 194) which confirms that the phase belongs to Magnetoplumb The XRD pattern consists of standard reflecting planes (1 1 3), (1 0 7), (2 0 0), (2 0 1), (0 0 12), (3 0 4) and (2 2 0), which counter confirmed that the investigated sample bare single M – type phase. This is also confirmed from the standard JCPDS data file no. 27 – 1029 and no. 84 – 0757. Lattice constants 'a' and 'c' for the samples were calculated from the observed interatomic spacing and found to be in the range 5 - 6 Å and 22 - 23 Å respectively as reported elsewhere [13].

In the present case the lattice constant 'a' remains unchanged while 'c' has shown increment by 0.0062Å which can be interpreted from the ionic radii of Al (0.53 Å) and Cr (0.62 Å). Similar types of result were observed by Khobragade et. al.(2011), Deshpande et.al. (2012) [14, 11], however bulk density (ρ_M)of the powdered sample is much smaller than X ray density (ρ_x) indicating that it is highly porous material. During combustion process large amount of gases (like

Methane CH_4, Ammonia NH_3, Nitrogen N_2, Water vapour H_2O) are evolved which leads to enhance the porous nature of the sample. The replacement of Fe^{3+} ion by Al^{3+} or Cr^{3+} ion in the hexagonal crystal lattice leads to the variation of bonding and consequently interatomic distance and porosity [15]. The particle size of both samples were calculated from Scherer formula revels size in nanometer scale [16].

Fig.2: TEM images of (a) Sample $CaCr_1Fe_{11}O_{19}$ and (b) Sample $CaAl_1Fe_{11}O_{19}$

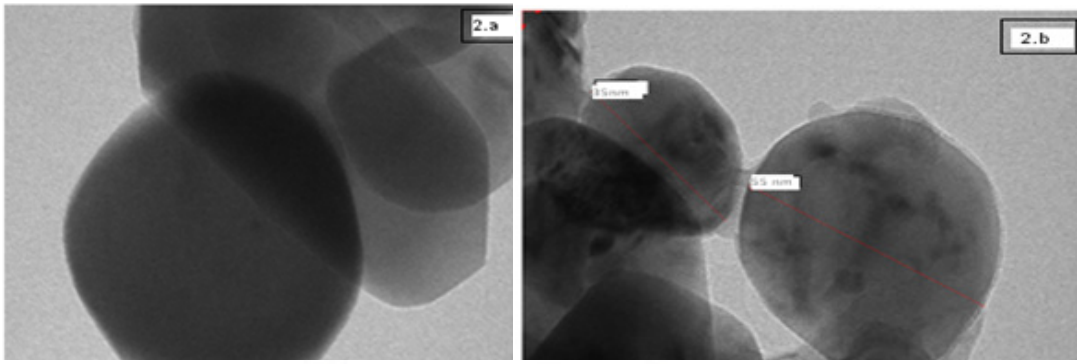

The TEM images of sample shows well crystallize particles possessing hexagonal shape with particle size ranges from 43 to 55nm respectively (fig 2). The SEM micrographs also confirms that the particle size ranges from 43 to 55nm respectively in fig.3

Fig.3: SEM micrographs of (a) Sample $CaCr_1Fe_{11}O_{19}$ and (b) Sample $CaAl_1Fe_{11}O_{19}$

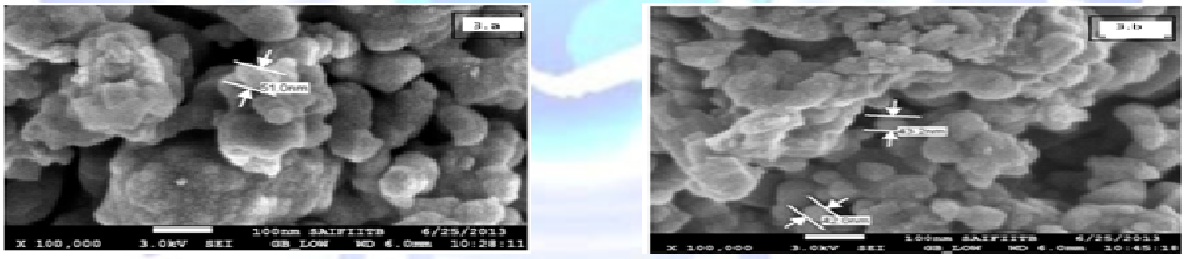

The magnetization curves are depicted in fig.(4a and 4b) for $CaAl_1Fe_{11}O_{19}$ (CAM) and $CaCr_1Fe_{11}O_{19}$ (CCM) which shows hysteresis indicating a hard magnetic properties with coercivity (Hc) varies between 1000 to 3400 Oe for both the samples. This data (Table 3) have reasonable agreement to the previous report by Teh and Jaferson 2002 [17].The saturation magnetization measured at 20 kOe field as a function of dopant at room temperature lies between 14 to 68 emu/g, which is lower than the reported polycrystalline samples [18] and is probably due to staking defects of RS block along the c-axis. This saturation magnetization can be explained as $Fe^{3+}/(Al^{3+}, Cr^{3+})$ ions per formula unit are on spin down position replacing Fe^{3+} ions having magnetic moment to be 5μB Probably in powder grains there exists small domains invisible while using X-rays where rich calcium blocks have been substituted for R-block magnetization of M-type hexaferrites is smaller than antiferromagnetic block and therefore the mean magnetization is weak Kalogiron et. al. 1991 [19]. In hexaferrites the interaction between two closed sites such as 2a – 12k, 2a – $4f_1$ and 2b – 12k is decisive for strong magnetic character, whenever magnetic ions are present in these sites strengthening or weakening of

super exchange interaction produces an increase in the magnetic characteristics [20] . The main governing factor in this compound are that they contains Al^{3+} or Cr^{3+} ions whose magnetic moment is zero which is less than Fe^{3+} (5μB), which have high magnitude of exchange interaction, particularly when all sites are filled by magnetic ions. The result shows that the Fe (12k) sub lattice making link among octahedral RS- structural block is subjected to very competitive exchange interaction , so that when Fe^{3+} ions in the 12k sub lattice are replaced by non magnetic (Al^{3+}, Cr^{3+}) weakening of super exchange interaction between the magnetic ions result in fairly inclined ferrimagnetism. From the magnetization curve the squarness (SQR) ratio (Mr/Ms) is determined which is less than 0.5. In general for ferrites the value of SQR if exists below 0.5 then it is good for recording medium.

Table No. 3: Magnetic parameters from Hysteresis loops.

Composition	Saturation Magnetization Ms (emu/g)	Remanent Magnetization Mr (emu/g)	Coercivity Hc (Oe)	Remanence Ratio=Mr/Ms
$CaAl_1Fe_{11}O_{19}$	67.765	28.009	3386.1	0.4133
$CaCr_1Fe_{11}O_{19}$	14.804	03.1922	1045.00	0.2026

Figure (4) shows the BH curve measurement at room temperature in the range of 15kOe, from which saturation magnetization (Ms), retentivity (Mr), Coercivity (Hc), squareness ratio (Mr/Ms) is determined. From the linear regration formula calculated by using Gorter's Co-linear model, assuming spin of the ions in the 2a, 2b and 12k positions alligned parallel to crystallographic c – axis whereas those in $4f_1$ and $4f_2$ positions oriented antiparallel to the former. The saturation magnetization of polycrystalline sample for CCM is 8.63 μB/fu which is smaller than 18.8 μB measured on single crystal of CaM while for CAM it is 19.14 μB/fu which is larger than 18.8 μB. The lower value of Ms observed on polycrystalline sample in CCM is probably due to stacking defects of R-S Blocks along c-axis. The decrease in the coercivity (Hc) of CCM can be explained by change of anisotropy constant K_1 since Hc is related to K_1 by Stoner – Wohlfarth expression [21]. $Hc = \alpha K_1/Ms$, where α – represents geometrical parameter. Another reason for reduction of coercivity is extrinsic effect which causes increase in grain size with substitution. SEM morphology (fissure 3)also depicts same variations.This effect is authenticated by the fact that coercivity is inversely proportional to grain size.

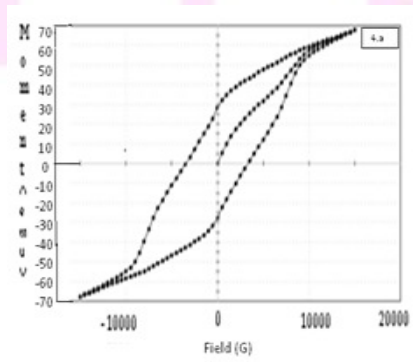

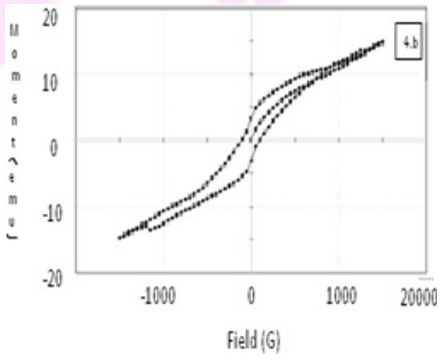

Fig 4(b) M–HCurveForCaCr$_1$Fe$_{11}$O$_{19}$

The grain size of Al–substituted hexaferrites are finer than Cr substituted hexaferrites which may lead to increase in the value of Hc, this resembles with the report by Mendoza Swartz et. al. 2003 [22]. In CAM the Hc is higher than CCM in the view of the fact that the particle shape is thin plate (Figure.2), the demagnetization

coefficient in the easy c-axis direction is set based on the condition of energy equilibrium for the assembly of randomly oriented particles. It is probable that the higher value of Al^{3+} substitution promotes to the higher roasting temperature necessary to improve ferrite crystallinity. This leads to the enhancement in the value of coercivity (Hc) in CAM.

The value of retentivity (Mr) and coercivity (Hc) is higher in CAM than that of CCM. The strong increase in retentivity (Mr) and coercivity (Hc) demonstrate that some inter-sub lattice exchange interactions are dominant and can be seen that the spin co-linearity appears mostly in spin up sub lattice: especially the 12k sub lattice have degree of frustration being in this way strongly detected by increase of 12k – $4f_1$ interaction from mean field analysis of the exchange interaction in CAM hexaferrites [23]. The result shows that Fe (12k) sub lattice, making link among octahedral R-S structural blocks subjected to very strong competitive reaction. So when Fe^{3+} ions in the 12k sub lattices are replaced by low magnetic ions results in weakening of the super exchange magnetic ions results in fairly inclined ferrimagnetism.

4. Conclusions:

The precursor of M – type hexagonal nano-hexaferrites with single domain were prepared by sol – gel auto-combustion method. The average particle size ranges between 45-55nm measured from transmission electron micrographs. Effects of Cr and Al substitution on Fe crystallographic sites on structural and magnetic properties of calcium nanoferrite are reported. It is clear that saturation magnetizations are closely related to the distribution and concentration of Cr^{3+} and Al^{3+} ions occupy octahedral 12k sites, with Cr^{3+} entering the Fe^{3+} crystallographic sites, the saturation magnetization dramatically falls but coercivity retains fair value. The decrease of magnetization is therefore attributed to Cr^{3+} ions occupying on the spin up Fe^{3+} sites (12k site) and magnetic dilution or non collinear structure. It is evident that Fe^{3+} - O - Fe^{3+} super exchange interaction may be weakened by Cr^{3+} ($3d^3$) substituting in to some Fe ($3d^5$) sites. Furthermore, the increase in coercivity is due to finer grains.

5. References:

1. J. Wang, P .F .Chong, S. C. Ng, L. M. Gan, Mater. Lett. 30, 217, 1997.
2. B. S. Satone, A. S. Kakde, M. J. Gothe, K. G. Rewatkar, P. S. Sawadh, International Journal of Researches in Biosciences, Agriculture and Technology, Vol. 1(2), 949 – 955, 2014.
3. M.M. Costa, G.F.M. Pires Junior, A.S.B. Sombra., International Journal of Materials Chemistry and Physics, 123, 35–39, 2010.
4. R. M .Sanshetti, Vahiremath, V.M.Jali., Bull. Matter. Sci, Vol 34, 5, 1027-1031, 2011.
5. A. M. Bhavikatti, S. Kulkarni, A. Lagashetty, International Journal of Engineering Science and Technology Vol. 2(11), 6532-6539, 2010.
6. E. W. Gorter., IEEE Trans. 1043, 1957 – 255, 1957.
7. X. Z. Zhou, A. H. Morrish, Z. W. Li and Y. K. Hang, IEEE Trans. Magn. Mag-27, 4654 1991.
8. S. Iel Park, S. Wha Lee and C. Sung Kim., J. Korean Phys. Soc. Vol 31,193- 196, 1997.

9. M. N. Giriya, C. L. Khobaragade, K. G. Rewatkar, R.P. Tandon., International Journal of Scientific & Engineering Research, Volume 3, 10, 2012.
10. S.A.Pawade, K. G. Rewatkar, V. M. Nanoti., International Journal of Knowledge Engineering, Vol. 3, No. 1, 31–35, 2012.
11. A. Deshpande, S.N. Sable, V.M. Nanoti, K.G. Rewatkar., International Journal of Knowledge Engineering, Vol 3, Issue1, 140-142, 2012.
12. D. S. Bhoumik, N. M. Patil, K. G. Rewatkar., International Journal of emerging Technology and Applications in Engineering, Tech. and Sciences, Vol 4, 1, 29–32, 2012.
13. S. N. Sable, K. G. Rewatkar, V.M. Nanoti ., International Journal of Material Science and Engineering – B, Vol 168, 156 – 160, 2010.
14. L. Khobragade, Journal Materials & Metallurgical Engg., Vol 1, 1-12, 2011.
15. J. Abbas., Procedding of sixth international symposium on advanced materials, 155, 1999.
16. B. Parvatheeswara Rao, O. F. Culton., Journal of Optoelectronics and advanced Materials Vol 3, 991-994, 2006.
17. G. B. Teh, D. A. Jefferson., Journal of Solid state chemistry., 167, 254-257, 11, 2002.
18. K. G. Rewatkar, N. M. Patil, S. R. Gawali., Bull. Mater. Sci. Vol 28, No. 6, 2005.
19. O. Kalogirou, G. Haack, B. R. Rohl, W. Gunber., Solid state ionics 528, 63–65, 1993.
20. K. G. Rewatkar, N. M. Patil, S. Jaikumar, D. S. Bhowmik, M. N. Giriya, C. L. Khobragade., Journal of magnetism and magnetic materials., 316, 19-22, 2007.
21. E. C. Stoner, F. R. S. Wohlfarth and E. P. Wolhfarth., Phil Trans A 240 ,599, 1948.
22. G. Mendoza-Suárez, L. P Rivas-Vázquez, J. C. Corral-Huacuz, A. F. Fuentes., J. I. Escalante-García .,Physica B, 339:110–8, 2003.
23. A. Isalgue, A. Labarta, J. Tejeda, X. Obradors, Appl. Phys. A39, 221, 1986.